**ARTICLE**　　　　　　　　　　　　　　　　　　　　　　　　　**Open Access**

# Long non-coding RNA linc00645 promotes TGF-β-induced epithelial–mesenchymal transition by regulating miR-205-3p-ZEB1 axis in glioma

Chenlong Li[1], Hongshan Zheng[1], Weiliang Hou[1], Hongbo Bao[1], Jinsheng Xiong[1], Wanli Che[1], Yifei Sun[1], Haiming Sun[2,3] and Peng Liang[1]

## Abstract

Accumulating evidence indicates long noncoding RNAs (lncRNA) play a vital role in tumor progression. However, the role of linc00645-induced accelerated malignant behavior in glioblastoma (GBM) remains unknown. In the present study, linc00645 expression was significantly upregulated in GBM tissues and cell lines. High level of linc00645 was associated with poor overall survival in GBM patients. Knockdown of linc00645 suppressed the proliferation, stemness, migration, invasion, and reversed transforming growth factor (TGF)-β-induced motility of glioma cell lines. Furthermore, linc00645 directly interacted with miR-205-3p and upregulated of miR-205-3p impeded efficiently the increase of ZEB1 induced by linc00645 overexpression. Moreover, knockdown of linc00645 significantly suppressed the progression of glioma cells in vivo. miR-205-3p was a target of linc00645 and linc00645 modulates TGF-β-induced glioma cell migration and invasion via miR-205-3p. Taken together, our findings identified the linc00645/miR-205-3p/ZEB1 signaling axis as a key player in EMT of glioma cells triggered by TGF-β. These data elucidated that linc00645 plays an oncogenic role in glioma and it may serve as a prognostic biomarker and a potential therapeutic target for the treatment of glioma in humans.

## Introduction

Over the past few decades, glioma has been the leading cause of central nervous system malignant tumor-related deaths in China and worldwide[1]. Despite encouraging progress in the diagnosis and treatment, the prognosis of patients with glioma remains poor, with a median overall survival of 12–14 months[2]. The growing incidence and high fatality of glioma made it particularly urgent to elucidate the pathological mechanisms underlying its progression. It is well known that the process underlying the occurrence of glioma is complicated, involving a lot of genetic mutations and multiple steps of biological processes[3].

Epithelial-to-mesenchymal transition (EMT) is a well-recognized integral component of invasion and migration processes[4], which is characterized by loss of cell adhesion, changing in the composition of the cytoskeleton and acquisition of migration ability and invasive traits[5–7]. TGF-β is a crucial cytokine implicated in EMT, which activates EMT-related factors, such as zinc-finger transcriptional factors (Snail, Slug and ZEB1/2), Twist, α-smooth muscle actin (α-SMA) and ZEB1/2[8–11].

Long noncoding (lnc)RNAs are a class of RNA transcripts, >200 nucleotides in length, without protein-coding ability[12]. lncRNAs were previously considered as transcriptional noise; however, they have now been found to play key roles in a series of biological processes, such as epigenetic regulation, histone modification, transcriptional control, and RNA metabolism[13,14]. In particular,

Correspondence: Haiming Sun (sunhm@ems.hrbmu.edu.cn) or Peng Liang (liang_pengses@yahoo.com)
[1]Department of Neurosurgery, Harbin Medical University Cancer Hospital, Harbin, Heilongjiang 150001, P.R. China
[2]Laboratory of Medical Genetics, Harbin Medical University, Harbin, Heilongjiang 150001, P.R. China
Full list of author information is available at the end of the article.
Edited by B. Zhivotovsky

SPRINGER NATURE
CDDpress

several lncRNAs are considered to be critical regulators of tumor progression, such as MALAT1[15], HOTAIR[16], SChLAP1[17], ANRIL[18], TUG1[19], and ZEB1-AS1[20]. lncRNA H19, CCAT2, and HOTTIP has been found to be associated with EMT and poor patient prognosis in glioma[21–23]. However, the molecular mechanisms and potential biological role of lncRNA-mediated EMT remain largely unclear.

Long intergenic nonprotein coding RNA 645 (linc00645), which is located in human chromosome 14, is a newly identified lncRNA found to be oncogenic in endometrial cancer[24]. Chen et al.[24] first identified linc00645 by sequenced the lincRNA transcriptome of endometrial cancers and then the author found that linc00645 was upregulated in endometrial cancer and demonstrated exquisite specificity for malignant endometrium, which may utility as biomarkers of malignant pathology. Liang et al.[25] identifed the increased level of linc00645 through a combination of WGCNA, univariate Cox regression analysis, and LASSO PH model. Moreover, a lncRNA-based risk scoring system was constructed and showed Linc00645 may be related to focal adhesion, extracellular matrix receptor interaction, and mitogen-activated protein kinase signaling pathways, as well to poor prognosis in glioblastoma (GBM). This indicates that the linc00645 is a promising prognostic biomarker for GBM and may play important roles in tumorigenesis of GBM.

Recently, a number of studies have proven that lncRNAs act as ceRNAs to regulate EMT through impeding target miRNAs and indirectly regulating the miRNA target genes in biological events[26–30]. We investigated and performed a mechanistic analysis to determine how linc00645 modulates cell proliferation, invasion and migration. Taken together, these findings demonstrated the role of linc00645 in the progression of glioma and may point to a new treatment strategy for glioma.

## Results

### Aberrant expression and prognostic significance of linc00645 in glioma patients

In this research, we first explored the expression level of the lncRNA by collecting the data from TCGA and GEO database. For the normalized gene expression profile data, we used the edge R package of R software to analyze significantly aberrantly expressed lncRNAs at the level: moderately to GBM samples vs. normal samples[31]. We selected a log fold change > 2 and false-discovery rate (P value) < 0.01 as significantly cutoff values based on the Benjamini–Hochberg method[32]. Then top 200 differentially expressed lncRNAs meeting the criteria from TCGA and GEO databse were collected respectively. FunRich (http://www.FunRich.org) was used to detect the overlapping lncRNAs among GSE4290 and TCGA.
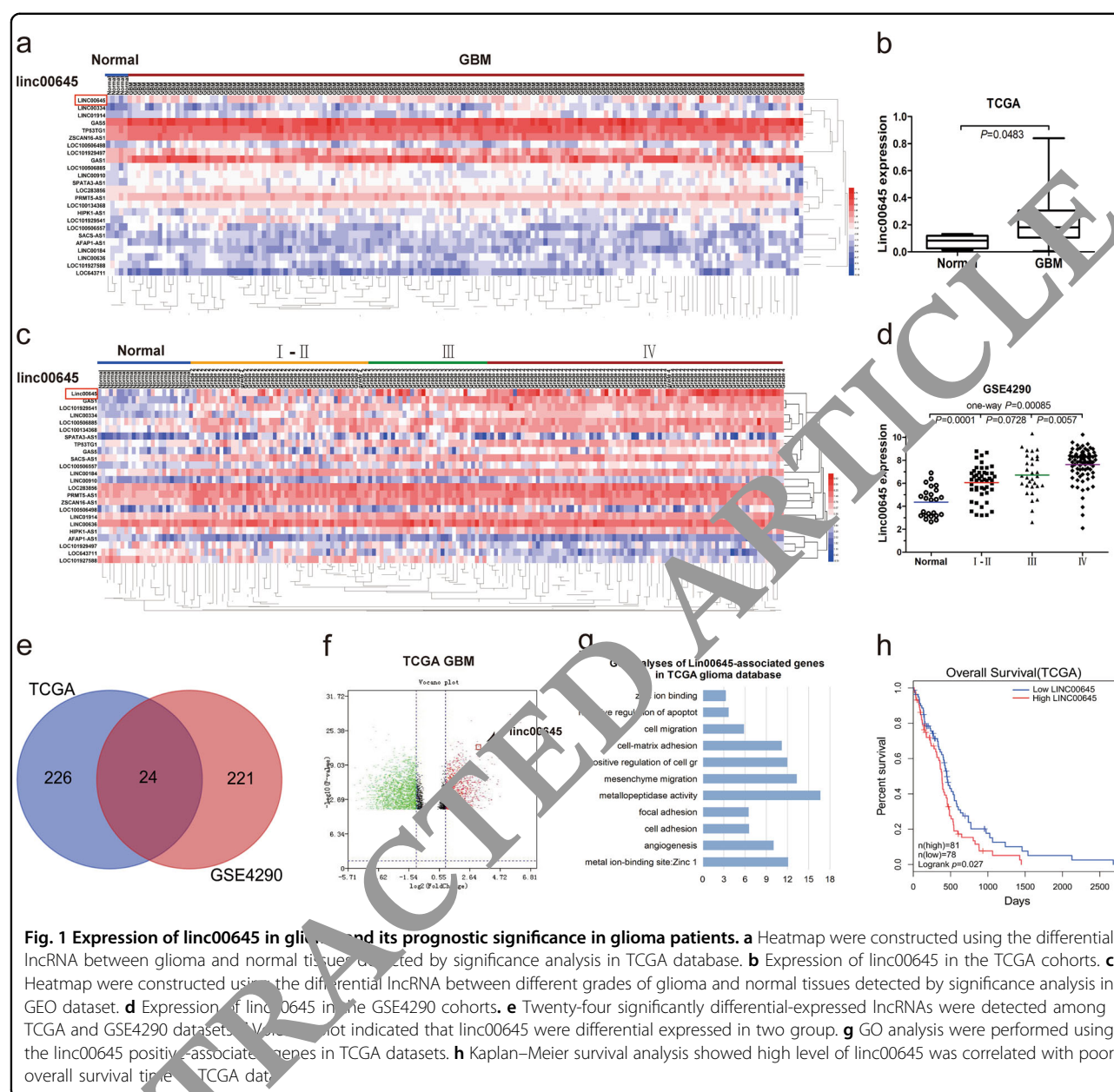
We generated Venn diagram by FunRich to visualize the intersecting lncRNAs between the results of two comparisons for further analysis (Fig. 1e). Then 24 intersecting lncRNAs between the results of two comparisons were obtained and these lncRNAs were identified according to the level of log fold change and displayed in Fig. 1a–d. We noticed that linc00645 was markedly upregulated in glioma tissues and the differentially expressed level of linc00645 is the most significant in both GSE4290 and TCGA datasets. The volcano plot demonstrated that GBM patients showed high-level of linc00645 expression differences in TCGA dataset (P = 0.008; Fig. 1f). These results indicated a significant increase of linc00645 level compared with normal brain tissue and a positively correlation with the pathological grade of glioma in CGGA, and GEO datasets (Fig. 1a–c and Additional file 1: Fig. S1a).

To further investigate the functions activated by linc00645, we analyzed the expression profiles of associated genes using data collected from the Gene Ontology (GO) database. The most prominent GO biological processes mainly included cell migration, adhesion, and zinc ion binding (Fig. 1g). Moreover, TCGA and CGGA data revealed that high level of linc00645 in patients with glioma was correlated with poor overall survival (Fig. 1h and Additional file 1: Fig. S1b). These results indicate that linc00645 may act as an oncogene and play a key role in glioma development.

### Knockdown of linc00645 suppresses the malignant behavior of glioma cells

The linc00645 expression level was then confirmed in 50 GBM tissues and adjacent normal brain tissues (NBTs) and 5 glioma cell lines (U251, T98G, LN229, A172, and SHG44). Compared with the normal human astrocyte (NHA) cell line by conducting quantitative reverse transcription polymerase chain reaction (qRT-PCR) analysis. The linc00645 expression levels in glioma tissues and glioma cell lines were found to be significantly increased compared with those in normal tissues and NHA cell line (Fig. 2a, b). We then investigated the association between linc00645 overexpression and clinicopathological characteristics in 50 GBM samples. The results showed that linc00645 overexpression was significantly associated with gender and mean tumor diameter (Table 1). Kaplan–Meier survival analysis revealed that higher linc000645 mRNA level was correlated with poor overall survival in GBM patients (P = 0.0034, log-rank test, Fig. 2c).

To investigate the biological function of linc00645 in glioma, we employed two cell lines highly expressing linc00645 (U251 and T98G) and one low linc00645 expression cell line (LN229) for further experiments. Subsequently, we designed three different linc00645 short

**Fig. 1 Expression of linc00645 in glioma and its prognostic significance in glioma patients. a** Heatmap were constructed using the differential lncRNA between glioma and normal tissues detected by significance analysis in TCGA database. **b** Expression of linc00645 in the TCGA cohorts. **c** Heatmap were constructed using the differential lncRNA between different grades of glioma and normal tissues detected by significance analysis in GEO dataset. **d** Expression of linc00645 in the GSE4290 cohorts. **e** Twenty-four significantly differential-expressed lncRNAs were detected among TCGA and GSE4290 datasets. **f** Volcano plot indicated that linc00645 were differential expressed in two group. **g** GO analysis were performed using the linc00645 positive-associated genes in TCGA datasets. **h** Kaplan–Meier survival analysis showed high level of linc00645 was correlated with poor overall survival time in TCGA data

interfering RNAs (siRNAs) and one overexpression plasmid for transfection into the above mentioned cell lines. As shown in Fig. 2d, of the three siRNAs, si-linc 1# and 3# exhibited the best efficiency. In order to reduce the risk of off-target effects, we selected si-linc 1# and 3# for the following experiments. In addition, we constructed linc00645 overexpression vector using pcDNA3.1, and found that the linc00645 expression level was significantly upregulated following transfection in LN229 cells (Fig. 2e). Furthermore, linc00645 expression was measured in nuclear and cytoplasmic fractions from three glioma cell lines (U251, T98G, and LN229). As shown in Fig. 2f, linc00645 was localized mainly in cytoplasm, indicating

that linc00645 may exert both transcriptional and post-transcriptional regulatory effects on glioma cell lines.

Since lncRNAs may participate in various biological processes, the following experiments were conducted to investigate the role of linc00645 in glioma. As shown in Fig. 2g, MTT assay demonstrated that the cell proliferation capacity was significantly reduced in cells transfected with si-linc1# and 3#. Furthermore, the colony formation assays revealed that linc00645 knockdown was associated with decreased clone number and size compared with the NC group in U251 and T98G glioma cells (Fig. 2h). The apoptosis assay revealed that linc00645 knockdown slightly increased apoptosis in T98G cells, but not in
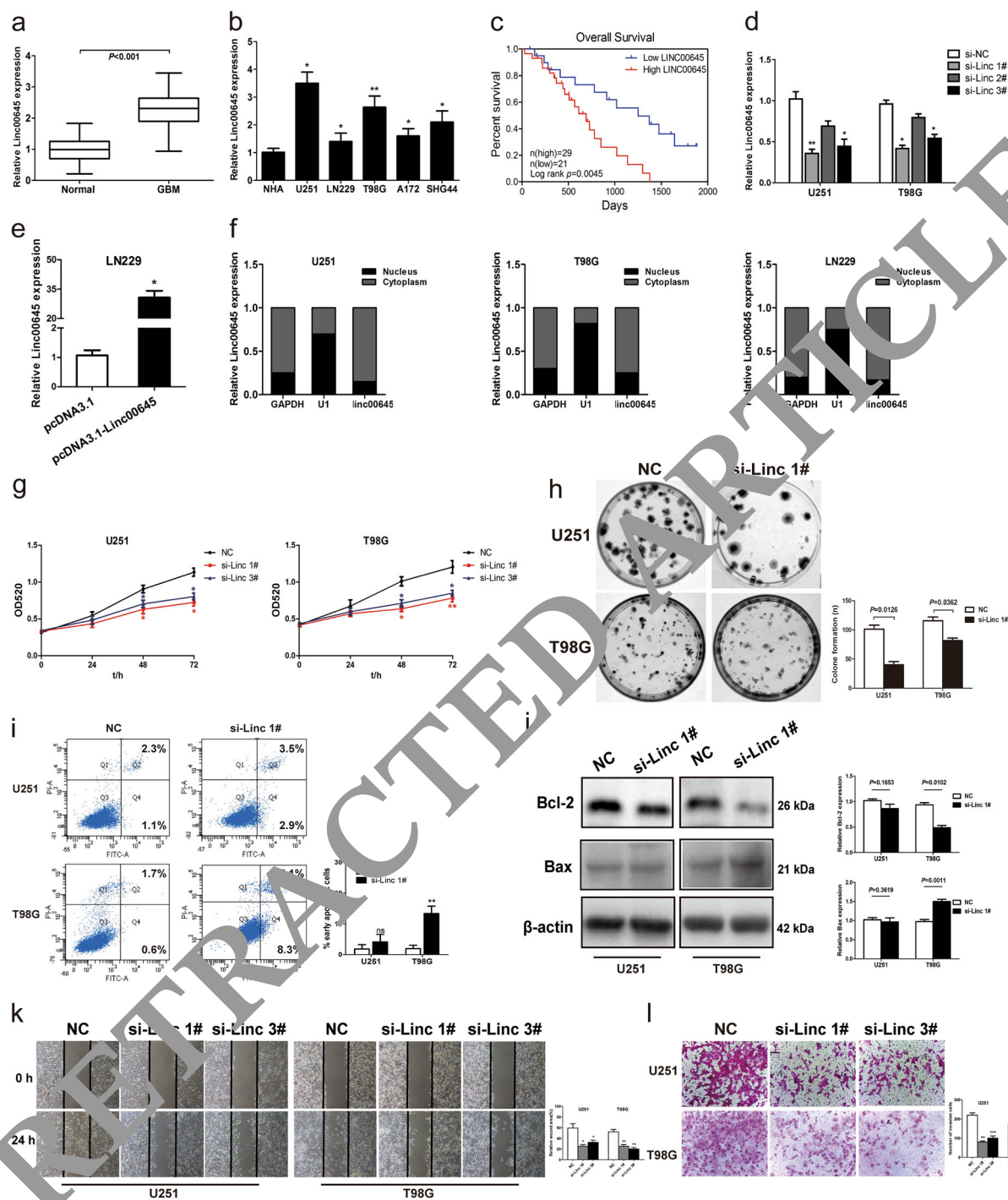
**Fig. 2 Effect of linc00645 on glioma cell proliferation, migration and invasion of glioma cells in vitro. a, b** qRT-PCR analysis indicated high level of linc00645 in glioblastoma tissues (n = 50) and glioma cell lines. **c** Kaplan-Meier algorithm showed high linc00645 was correlated with poor overall survival in 50 patients with GBM (log-rank test). **d** Linc00645 expression was efficiently knocked down by siRNAs in U251 and T98G cells as detected by qRT-PCR assays. **e** Ectopic expression of linc00645 in linc00645-transfected LN229 cells was determined by qRT-PCR. **f** Linc00645 expression levels in different subcellular fractions cells were measured by qRT-PCR in U251, T98G and LN229 cells. Black range indicates nuclear fraction, Gray range indicates cytoplasmic fraction. **g** MTT assay in si-NC or si-Linc 1# transfected U251 and T98G cells. (*$P < 0.05$, **$P < 0.01$, independent Student's t test). **h** Colony formation assay in si-NC or si-Linc 1# transfected U251 and T98G cells. **i** Effect of linc00645 knockdown on U251 and T98G cell apoptosis. The apoptosis rate was displayed with bar graph. **j** Expression of Bcl-2 and Bax in si-NC or si-Linc 1# transfected cells as detected by western blot. The protein level was displayed with bar graph. **k, l** si-Linc 1# may inhibit migration and invasion ability in U251 and T98G cells. Data are shown as the mean ± SD of three independent experiments. (*$P < 0.05$, **$P < 0.01$)

**Table 1 Correlation between the expression of linc00645 and the clinicopathological feature in glioma tissues**

| Variables | No. of cases | Linc00645 expression | | $\chi^2$ | P value |
|---|---|---|---|---|---|
| | | Low | High | | |
| *Age, years* | | | | 2.122 | 0.145 |
| <60 | 18 | 10 | 8 | | |
| ≥60 | 32 | 11 | 21 | | |
| *Gender* | | | | 9.425 | **0.002*** |
| Male | 27 | 6 | 21 | | |
| Female | 23 | 15 | 8 | | |
| *Karnofsky, KPS* | | | | 2.313 | 0.128 |
| <60 | 30 | 10 | 20 | | |
| ≥60 | 20 | 11 | 9 | | |
| *Mean tumor diameter (cm)* | | | | 5.476 | **0.019*** |
| <5 | 26 | 15 | 11 | | |
| ≥5 | 24 | 6 | 18 | | |
| *Necrosis on MRI* | | | | 0.011 | 0.917 |
| Yes | 29 | 12 | 17 | | |
| No | 21 | 9 | 12 | | |
| *Seizure* | | | | 0.006 | 939 |
| Yes | 14 | 6 | 8 | | |
| No | 36 | 15 | 21 | | |

*$P < 0.05$ was considered significant ($\chi^2$ test between two groups)

U251 cells. Consistently, Bcl-2 was decreased while Bax was increased following linc00645 knockdown in T98G cells (Fig. 2i–j).

We then investigated whether linc00645 affected glioma cell migration and invasion capacities. The wound healing assay revealed that cells transfected with si-linc1# and 3# exhibited reduced migration (Fig. 2k). The Transwell assay also demonstrated decreased cell invasion capacity following downregulation of linc00645 expression (Fig. 2l). Conversely, overexpression of linc00645 enhanced the migration and invasion abilities in U251 and T98G cells (Additional file 1: Fig. S1c, d).

### Knockdown of linc00645 inhibits ZEB1 expression and impedes TGF-β-induced migration and invasion process in glioma cells

Accumulating evidence indicates that the TGF-β signaling pathway plays a key role in EMT induction in various types of cancer[33,34]. In the present study, 5 ng/mL TGF-β was found to be sufficient in inducing EMT (Fig. 3a and Additional file 2: Fig. S2a), while the TGF-β receptor antagonist SB431542 could inhibit the EMT
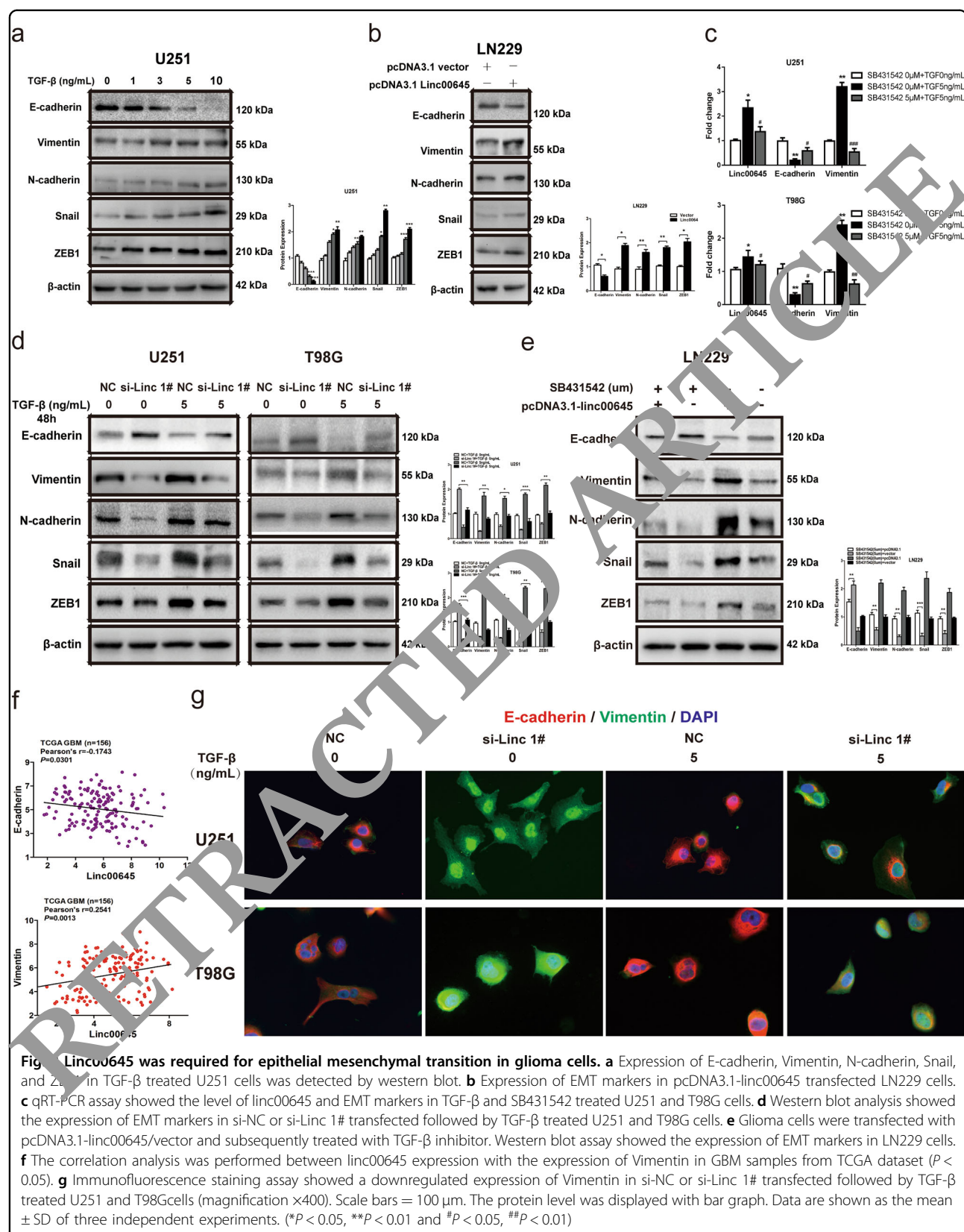
phenotype in U251 and T98G cells (Additional file 2: Fig. S2b). By contrast, overexpression of linc00645 promoted EMT in LN229 cells (Fig. 3b). linc00645 expression was significantly increased by TGF-β in U251 cells, but only slightly increased in T98G cells, and it was blocked by SB431542 (Fig. 3c). These results indicate that linc00645 may be involved in TGF-β-induced EMT in glioma.

Then, the levels of EMT markers were altered in U251 an T98G cells, with upregulation of E-cadherin and downregulation of vimentin, N-cadherin, Snail, and ZEB1 following linc00645 knockdown (Fig. 3d and Additional file 2: Fig. S2g). Then the images were captured under a light microscope (100×). Control group exhibited cobblestone-like character, while the TGF-β (+) group displayed spindle-like mesenchymal phenotype. But after co-cultured with TGF-β and si-linc 1#, the spindle-like mesenchymal phenotype was impeded. While overexpression of Linc00645 restored the expression of EMT-related markers when TGF-β is inhibited by SB431542 (Fig. 3e). And linc00645 may regulate EMT process in a TGF-β dependent manner. The results further supported that linc00645 modulates TGF-β-induced EMT process.

To verify the effects of linc00645 on EMT, we explored the expression levels of EMT markers and EMT-related transcription factors. The correlation of the linc00645 expression level with E-cadherin, vimentin, N-cadherin and ZEB1 was further investigated in the cohort of GBM samples from the TCGA database. The results verified that linc00645 expression was significantly correlated with the expression of E-cadherin ($R = -0.1743$, $P = 0.0301$), Vimentin ($R = 0.2541$, $P = 0.0013$), N-cadherin ($R = 0.2096$, $P = 0.0088$), and ZEB1 ($R = 0.2608$, $P = 0.0010$) (Fig. 3f and Additional file 2: Fig. S2c). In order to observe the switch of EMT process within glioma cells, we co-stained E-cadherin/Vimentin in U251 and T98G cells by immunofluorescence staining assays (Fig. 3g). Collectively, these results demonstrated that linc00645 is associated with EMT, which is a contributor to tumor metastasis in glioma.

### Correlation between linc00645 and miR-205-3p

Using miRDB and LncBase V2. database blast prediction combined with the data from TCGA, we found that linc00645 has several putative miRNA targets (miR-15-5p, miR-23a-3p, and miR-200a-3p). miR-205-3p had the highest score, and accumulating evidence indicates that miR-205-3p participates in EMT regulation by targeting ZEB1[35,36]. The potential binding sites of linc00645 were predicted by the bioinformatics databases (Fig. 4a and Additional file 2: Fig. S2d). The expression of miR-205-3p was downregulated in glioma tissues and glioma cell lines compared with normal brain tissues and NHA cell line (Fig. 4b, c). Then we found that the expression level of linc00645 was inversely correlated with the expression of
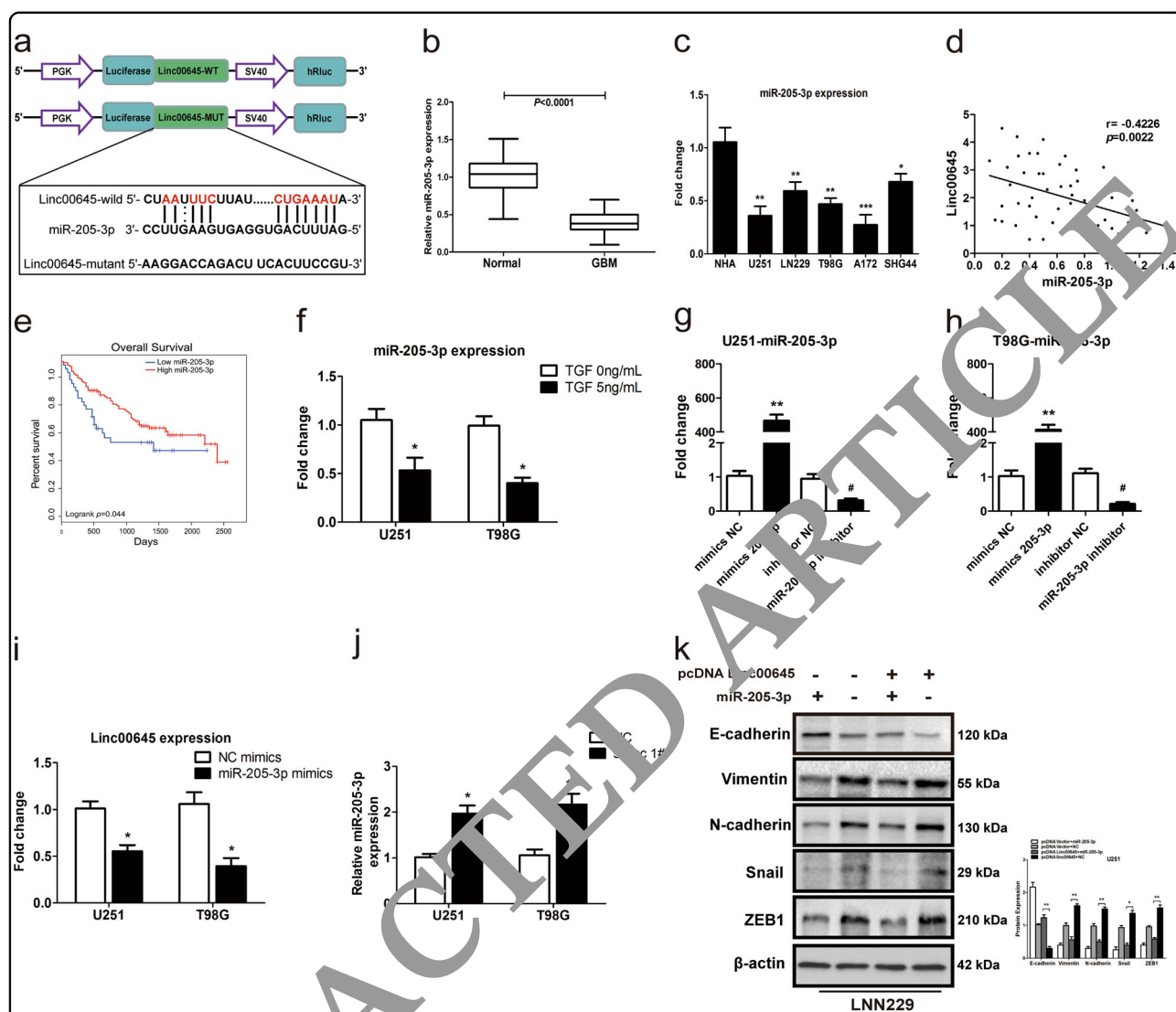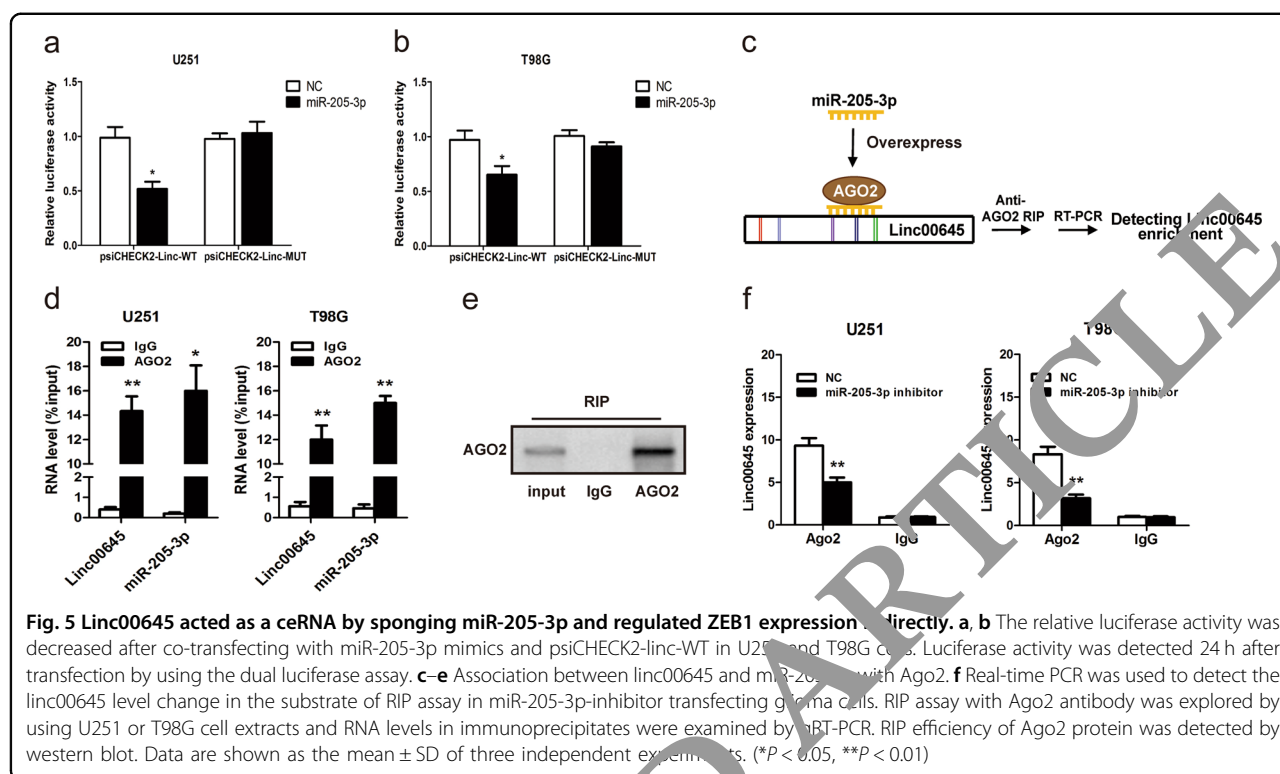
**Fig. Linc00645 was required for epithelial mesenchymal transition in glioma cells. a** Expression of E-cadherin, Vimentin, N-cadherin, Snail, and ZEB1 in TGF-β treated U251 cells was detected by western blot. **b** Expression of EMT markers in pcDNA3.1-linc00645 transfected LN229 cells. **c** qRT-PCR assay showed the level of linc00645 and EMT markers in TGF-β and SB431542 treated U251 and T98G cells. **d** Western blot analysis showed the expression of EMT markers in si-NC or si-Linc 1# transfected followed by TGF-β treated U251 and T98G cells. **e** Glioma cells were transfected with pcDNA3.1-linc00645/vector and subsequently treated with TGF-β inhibitor. Western blot assay showed the expression of EMT markers in LN229 cells. **f** The correlation analysis was performed between linc00645 expression with the expression of Vimentin in GBM samples from TCGA dataset (*P* < 0.05). **g** Immunofluorescence staining assay showed a downregulated expression of Vimentin in si-NC or si-Linc 1# transfected followed by TGF-β treated U251 and T98Gcells (magnification ×400). Scale bars = 100 μm. The protein level was displayed with bar graph. Data are shown as the mean ± SD of three independent experiments. (*$P$ < 0.05, **$P$ < 0.01 and #$P$ < 0.05, ##$P$ < 0.01)

**Fig. 4 Correlation between linc00645 and miR-205-3p. a** The predicted miR-205-3p binding sites on linc00645 and schematic of wild and mutant psiCHECK2-linc00645 constructs. **b, c** qRT-PCR analysis showed miR-205-3p was downregulated in glioblastoma tissues ($n = 50$) and glioma cell lines. **d** Pearson's correlation analysis indicated the negative relationship between linc00645 expression and miR-205-3p level in 50 glioma patients. **e** Kaplan–Meier analyses showed low miR-205-3p level was correlated with poor overall survival of glioma patients (The log-rank test was used to calculate $P$ value). **f** Expression of miR-205-3p was increased in TGF-β treated U251 and T98G cells. **g, h** The efficiency of miR-205-3p expression after glioma cells transfected with miR-205-3p NC, mimics, inhibitor NC and inhibitor. **i** After transfecting with miR205-3p mimics, the level of linc00645 was decreased in U251 and T98G cells as detected by qRT-PCR. **j** miR-205-3p was upregulated by linc00645 knockdown in U251 and T98G cells. **k** Western blot analysis showed the expression of E-cadherin, Vimentin, N-cadherin, Snail, and ZEB1 in miR-205-3p and pcDNA-linc00645 transfected U251 cells. The protein level was displayed with bar graph. Data are shown as the mean ± SD of three independent experiments. (*$P < 0.05$ and **$P < 0.01$, #$P < 0.05$)

miR-205-3p in human glioma tissues (Fig. 4d). The Kaplan–Meier curve demonstrated that a high level of miR-205-3p was positively correlated with the overall survival of patients with glioma (Fig. 4e). Furthermore, we observed that the miR-205-3p level was significantly reduced after TGF-β stimulation in U251 and T98G cells which indicating that upregulation of linc00645 may be associated with the decrease of miR-205-3p after treating with TGF-β (Fig. 4f)

The efficiency of miR-205-3p expression after glioma cells transfected with miR-205-3p mimics and inhibitor was identified by qRT-PCR assay (Fig. 4g, h). Then we focused on miR-205-3p and investigated the interaction between linc00645 and miR-205-3p in glioma tissues and cell lines. We then detected whether miR-205-3p could inhibit the expression of linc00645 in glioma cells. Indeed, increased miR-205-3p expression with miR-205-3p mimic could decrease the expression of linc00645 in U251 and

**Fig. 5 Linc00645 acted as a ceRNA by sponging miR-205-3p and regulated ZEB1 expression indirectly. a, b** The relative luciferase activity was decreased after co-transfecting with miR-205-3p mimics and psiCHECK2-linc-WT in U251 and T98G cells. Luciferase activity was detected 24 h after transfection by using the dual luciferase assay. **c–e** Association between linc00645 and miR-205 with Ago2. **f** Real-time PCR was used to detect the linc00645 level change in the substrate of RIP assay in miR-205-3p-inhibitor transfecting glioma cells. RIP assay with Ago2 antibody was explored by using U251 or T98G cell extracts and RNA levels in immunoprecipitates were examined by qRT-PCR. RIP efficiency of Ago2 protein was detected by western blot. Data are shown as the mean ± SD of three independent experiments. (*$P < 0.05$, **$P < 0.01$)

T98G cells (Fig. 4i). A reciprocal repression between MALAT1 and miR-205/miR-202 has been reported in cervical cancer cells and gastric cancer[37,38]. To investigate whether miR-205-3p was able to be negatively regulated by linc00645, we decreased the expression of linc00645 in glioma cells. The results suggested that miR-205-3p was upregulated by linc00645 knockdown in U251 and T98G cells (Fig. 4j). Then the effect on EMT was increased by overexpression of linc00645 in LN229 cells, which could be abolished by adding miRNA-205 to cells overexpressed linc00645 (Fig. 4k). These data confirmed that linc00645 and miR-205-3p reciprocally repress each other in glioma cells under both basal and stimulate conditions.

### miR-205-3p was a target of linc00645

lncRNAs act as endogenous miRNA sponges for binding to miRNA or participating in the competitive endogenous RNAs (ceRNA) regulatory network. Then, we subcloned full-length linc00645 (WT or MUT) into the downstream of firefly luciferase gene in psiCHECK2 vector (Fig. 4a). Further, co-transfection with the psiCHECK2-linc-WT luciferase reporter plasmid and miR-205-3p mimics reduced the reporter activity compared with the NC group in U251 and T98G cells (Fig. 5a, b). It is well-known that miRNAs function by interacting with RNA-induced silencing complex (RISC) that is required for miRNAs mediated gene silencing, and potential targets of miRNAs can be isolated from this

complex after Ago2 co-immunoprecipitation. Then we conducted RNA immunoprecipitation (RIP) assay with Ago2 antibody by qRT-PCR in U251 and T98G cells (Fig. 5c). As shown in Fig. 5d, e, compared with NC (Anti-IgG), linc00645 and miR-205-3p were both preferentially enriched in Ago2 antibody-incubated beads. And miR-205-3p inhibitor inhibited the interaction of AGO2 with Linc00645 in U251 and T98G cells (Fig. 5e). Consistently, these data indicated that linc00645 and miR-205-3p were in the same RISC complex and enriched in Ago2 in glioma cells.

As previously reported, miR-205-3p was found to directly target ZEB1 in several cancers, such as ovarian cancer, breast cancer, and oral squamous cell carcinoma[39]. To confirm these findings, we prepared psiCHECK2-ZEB1-3′UTR-WT or MUT luciferase reporter vector and then co-transfected it with miR-205-3p into glioma cells. The luciferase activity was measured and upregulation of miR-205-3p significantly decreased the luciferase activity compared with NC (Additional file 2: Fig. S2e, f).

Collectively, the above mentioned data indicate that miR-205-3p was a target of linc00645.

### Linc00645 modulates TGF-β-induced glioma cell migration and invasion via miR-205-3p

To identify the mechanisms underlying the inverse changes in linc00645 and miR-205-3p expression in

response to with or without TGF-β, we examined the regulatory relationship between linc00645 and miR-205-3p using gene overexpression and/or knockdown. Glioma cells were transfected with miR-205-3p mimics/NC or miR-205-3p inhibitor/inhibitor NC and subsequently treated with TGF-β. The data indicates that miR-205-3p overexpression inhibit linc00645 expression upregulated by TGF-β while miR-205-3p knockdown shows the opposite effects (Fig. 6a, b). These result confirm that miR-205-3p directly regulates linc00645 expression under both basal and stimulated conditions.

We observed that decreased protein levels of E-cadherin and increased Vimentin, N-cadherin, and ZEB1 were detected in glioma cells following TGF-β stimulation (Fig. 6c, d). A plausible explanation is that TGF-β treatment induced linc00645 expression, leading to downregulation of miR-205-3p and upregulation of its target ZEB1. miR-205-3p suppressed TGF-β-induced Vimentin, N-cadherin, and ZEB1 expression, and these changes were accompanied by increased E-cadherin level (Fig. 6c, d). These data supported the inhibitory role of miR-205-3p in TGF-β-induced EMT through downregulation of ZEB1. Linc00645 overexpression further restored the levels of ZEB1, as well as the EMT-related proteins Vimentin and N-cadherin downregulated by miR-205-3p (Fig. 6c, d). These results further support that linc00645 modulates TGF-β-induced EMT via miR-205-3p.

The hallmark of EMT is the loss of cell−cell adhesion and gain of migratory and invasive capacities. Our result indicated that, in alignment with increased EMT-related marker expression level, TGF-β treated glioma cells exhibited increased cell migration and invasion (Fig. 6e, f). Moreover, linc00645 knockdown further reduced cell migration and invasion increased by miR-205-3p inhibitor (Fig. 6e, f). Therefore, this evidence suggests that linc00645/miR-205-3p/ZEB1 signaling pathway play a key role in TGF-β-induced EMT process of glioma cells.

### Linc00645 knockdown regulated the ability of self-renewal and stemness and prompted differentiation in GSCs

To further explore the role of linc00645 in the stemness and self-renewal of CD133$^+$ glioma tumor stem cells (Fig. 7a). We investigated the self-renewal ability of linc00645 on neurosphere formation in U251 GSCs. qRT-PCR and Western blot assays demonstrated that linc00645 knockdown decreased the level of specific stemness markers, including Bmi-1, Oct-4, Sox-2, and Nanog (Fig. 7b, c). Subsequently, a significant decrease was detected in the volume and number of neurospheres transfected with si-linc 1# compared with NC group, indicating that linc00645 play a role in GSCs (Fig. 7d, e). Then the expression of stem cell marker (Nestin) and glial cells marker (GFAP) was examined in U251 GSC. These data confirmed that lin00645 knockdown decreased the

percentage of Nestin-positive cells and enhanced GFAP expression in glial differentiation (Fig. 7f, g). All these results suggested that linc00645 play a critical role in the maintenance of GSC stemness.
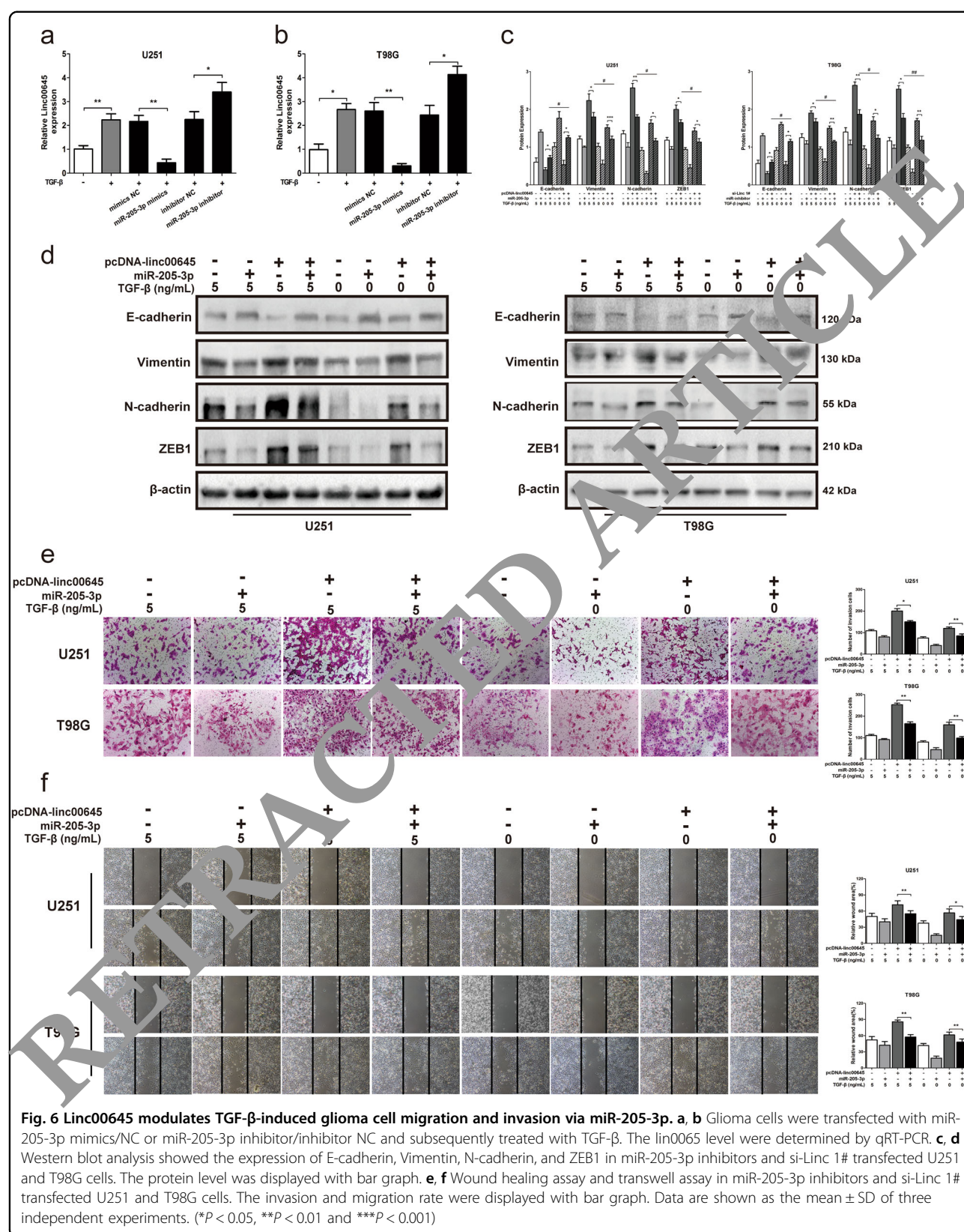
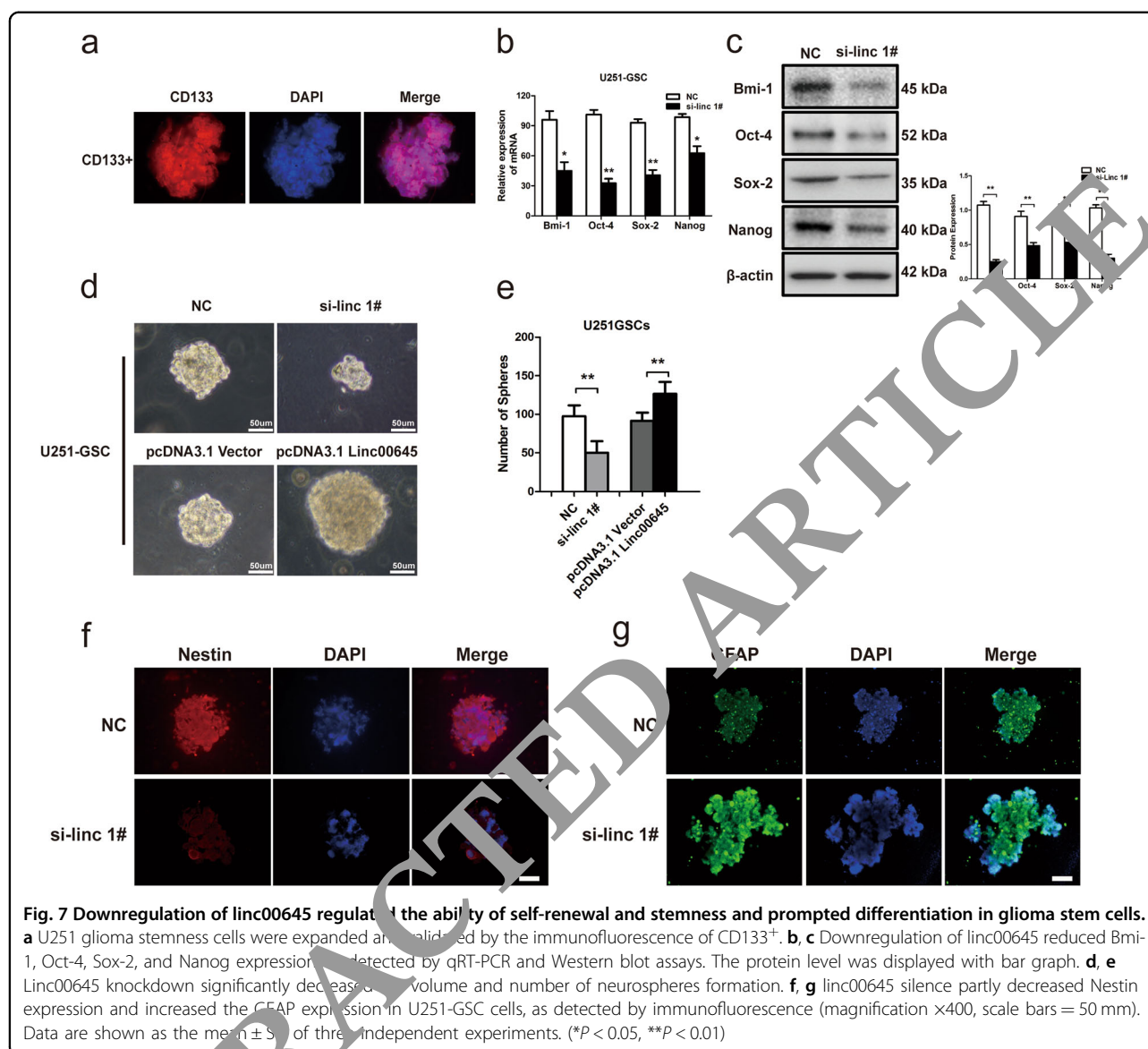### Linc00645 inhibition significantly suppressed tumor growth in vivo

To further assess the biological roles of linc00645 knockdown in vivo, an intracranial glioma model in nude mice was constructed. sh-NC or sh-linc00645 were intracranially inoculated with U251-luc cells into BALB/c nude mice. Whole-body bioluminescence imaging was employed to investigate the effect of sh-linc00645 on glioma tumor growth. The results revealed that linc00645 knockdown led to an obvious reduction in tumor formation ($P < 0.001$, Fig. 8a, c). H&E-stained coronal brain sections were obtained to show the tumor xenografts (Fig. 8b). Then qRT-PCR assay demonstrated that miR-205-3p expression was upregulated in the sh-linc00645 group (Fig. 8d). Moreover, linc00645-knockdown U251 cells exhibited decreased levels of ZEB1 (Fig. 8e). To further evaluate the inhibitory effect of sh-linc00645 on glioma development in nude mice, the survival time of each group ($n = 7$ per group) was evaluated by Kaplan–Meier curves, and the sh-linc00645-treated group exhibited a significant improvement in survival compared with the control group ($P < 0.05$; Fig. 8f).

### Discussion

Glioma is one of the leading causes of malignant central nervous system tumor-related deaths, and its prognosis remains poor[1,2]. In recent years, numerous studies reported the involvement of EMT or EMT(-like) mechanisms in increasing the malignancy of other nonepithelial tumors[7]. GBM tissues attributed to the mesenchymal subtype are characterized by significantly shortened event-free and overall survival[40]. And the recently defined mesenchymal subgroup of GBMs convincingly shows that the EMT(-like) process has clinical importance also in the case of malignant brain tumors[41]. And the molecular processes which increased tumor invasion, apoptosis resistance and cell migration in different tumors lacking the epithelial background, unequivocally regards EMT or EMT(-like) changes as an ubiquitous phenomenon with high clinical relevance[40].

Accumulating evidences have demonstrated EMT is initiated by transcription factors or external signals, such a ZEB, Snail, Slug, and TWIST[42]. In addition, an increasing number of lncRNAs have been identified as regulators of TGF-β signaling and EMT process. Padua et al. indicated that downregulation of Hotair expression suppressed the EMT process by TGF-β1 in breast cancer[43]. LncRNA XIST had been reported to play a role in regulating tumor metastasis in colorectal cancer[44]. It has

**Fig. 6 Linc00645 modulates TGF-β-induced glioma cell migration and invasion via miR-205-3p. a**, **b** Glioma cells were transfected with miR-205-3p mimics/NC or miR-205-3p inhibitor/inhibitor NC and subsequently treated with TGF-β. The lin0065 level were determined by qRT-PCR. **c**, **d** Western blot analysis showed the expression of E-cadherin, Vimentin, N-cadherin, and ZEB1 in miR-205-3p inhibitors and si-Linc 1# transfected U251 and T98G cells. The protein level was displayed with bar graph. **e**, **f** Wound healing assay and transwell assay in miR-205-3p inhibitors and si-Linc 1# transfected U251 and T98G cells. The invasion and migration rate were displayed with bar graph. Data are shown as the mean ± SD of three independent experiments. (*P < 0.05, **P < 0.01 and ***P < 0.001)

**Fig. 7 Downregulation of linc00645 regulated the ability of self-renewal and stemness and prompted differentiation in glioma stem cells.**
**a** U251 glioma stemness cells were expanded and validated by the immunofluorescence of CD133^{+}. **b, c** Downregulation of linc00645 reduced Bmi-1, Oct-4, Sox-2, and Nanog expression, detected by qRT-PCR and Western blot assays. The protein level was displayed with bar graph. **d, e** Linc00645 knockdown significantly decreased volume and number of neurospheres formation. **f, g** linc00645 silence partly decreased Nestin expression and increased the GFAP expression in U251-GSC cells, as detected by immunofluorescence (magnification ×400, scale bars = 50 mm). Data are shown as the mean ± SD of three independent experiments. (*P < 0.05, **P < 0.01)

been reported that lncRNAs participated in TGF-β signaling and the EMT process[45]. Lu et al.[46] suggested that linc00673 repressed the malignant biological cell behavior and EMT by sponging miR-150-5p. XIST was shown to promote TGF-β-induced EMT by regulating miR-367/141 in NSCLC[47].

A growing number of studies confirm that lncRNAs can also antagonize other noncoding RNAs, such as miRNAs, and miRNAs may also exert a regulatory effect on lncRNAs[48,49]. It has been previously reported that miR-205-3p suppresses proliferation and invasion of glioma cells[50,51]. Then we hypothesized that linc00645 inhibits the malignant behavior of glioma via interacting with miR-205-3p.

Recent studies reported that ncRNAs involved in the regulation of the epithelial phenotype and inhibition of

EMT, including several miRNAs, such as the miR-200 family, were verified to target ZEB1[39]. miR-205-3p has been reported to play a role in EMT process by inhibiting the expression of ZEB1 by binding the 3′UTR site[52]. ZEB1, one member of ZEB protein family, was considered as a transcriptional factor which cooperated with TGF-β signaling and downregulated the expression of E-cadherin. Furthermore, ZEB1 was found to promote EMT in tumor cells[42].

The crosstalk between miRNAs and TGF-β signaling mediated EMT process and tumor invasion has been demonstrated in many cancer types[53]. It has been reported that inhibition of SMAD3 by miR-145 and miR-203, and inhibition of SMAD4 by miR-205 can suppress TGF-β-induced EMT in NSCLC cells[54]. In the present study, we found that 205-3p represses TGF-β-induced EMT and
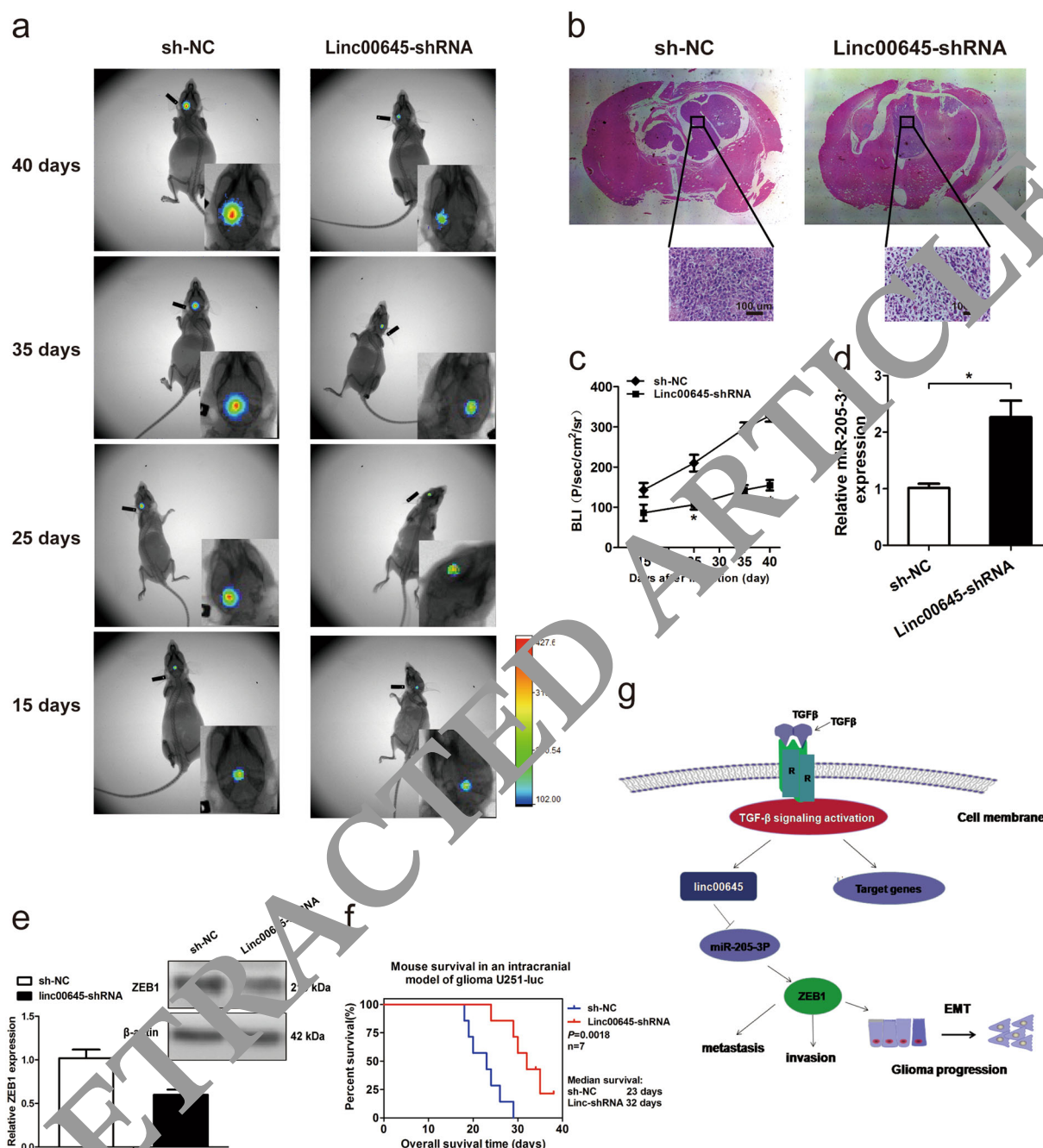
**Fig. 8 linc00645 knockdown suppressed tumor growth in vivo and prolonged survival. a**, **c** Luminescence imaging showed the BLI value of Linc00645-shRNA treated U251-luc glioma group was decreased compared with NC-shRNA group. The dynamic process of tumor proliferation was displayed with different time point (15, 25, 35, and 40 days). The line chart showed the change of tumor BLI value. **b** H&E-stained coronal brain sections showing representative tumor xenografts. **d** The level of miR-205-3p was enriched in Linc00645-shRNA intracranial graft group detected by qRT-PCR. **e** The expression of ZEB1 was reduced in Linc00645-shRNA intracranial graft group detected by Western blot. The protein level was displayed with bar graph. **f** Kaplan-Meier survival analysis indicating that mice transfected with linc00645-shRNA revealed a significantly better outcome than the sh-NC treated group. **g** The schematic overview of linc00645/miR-122/ZEB1 mediated EMT in glioma. Data are shown as the mean ± SD of three independent experiments. (*$P < 0.05$, ***$P < 0.001$)

glioma cell migration and invasion. More and more evidence suggested that miR-205 alone or together with miR-200 influenced cancer cell invasion mainly through TGF-β signaling and EMT[39]. These result are in agreement with ours study that miR-205-3p inhibit TGF-β-induced motility and invasion.

Linc00645 downregulated miR-205-3p by suppressing the expression of endoribonuclease DICER. miR-205-3p suppressed linc00645 expression by recruiting linc00645 to RISC for degradation. Linc00645 modulates TGF-β-induced EMT through regulation of miR-205-3p and its target genes ZEB1 (Fig. 8g).

In conclusion, our research indicated that high linc00645expresion predicted worse overall survival for glioma patients. Our findings identified the linc00645/miR-205-3p/ZEB1 signaling axis as a key player in EMT of glioma cells triggered by TGF-β. These results will improve our understanding of the mechanisms underlying cancer development and may provide a potential novel strategy for the treatment of human glioma.

## Materials and methods

### Cell culture and clinical samples

The human glioma cell lines U251, LN229, T98G, A172, and SHG44 were obtained from the Cell Bank of Chinese Academy of Sciences (Shanghai, China). Normal Human Astrocyte (NHA) cells were purchased from the American Type Cell Culture Collection (ATCC; Rockville, MD, USA). All cells were cultured in Dulbecco's modified Eagle's medium (DMEM; HyClone; GE Healthcare Life Sciences, Logan, UT, USA) with 10% fetal-bovine serum (Gibco; Thermo Fisher Scientific, Inc., Los Angeles, CA, USA) in a 37 °C, 5% $CO_2$ humidified atmosphere.

GBM samples and adjacent normal brain tissues were collected from 50 patients who underwent tumor resection at Harbin Medical University Cancer Hospital between December 2012 and December 2016 Additional file 3: Table. S1. GBM patients had not received radiotherapy or chemotherapy treatment prior to surgery. All tissue samples were pathologically confirmed and immediately snap-frozen in liquid nitrogen until RNA extraction. Written informed consent to the use of the tissue samples for research purposes was obtained from each patient. All procedures were conducted in accordance with the principles outlined in the Declaration of Helsinki, and all applicable international, national and/or institutional guidelines for the care and use of animals were followed. The study protocol was approved by the Ethics Committee of Harbin Medical University (Harbin, China).

### Sphere formation assay

The U251 glioma stem cell (GSC) cells were cultured in serum-free DMEM supplemented with B-27 (Gibco; Thermo Fisher Scientific, Inc., NY, USA), 20 ng/ml basic fibroblast growth factor (bFGF; Sigma-Aldrich; Merck KGaA, St. Louis, MO, USA) and 20 ng/ml epidermal growth factor (EGF; Sigma-Aldrich; Merck KGaA). The cells were suspended in ultra-low attachment surface 6-well culture plates (Corning Inc., Corning, NY, USA). The medium was changed every 3 days. The number of neurospheres was counted under a light microscope (Nikon Corp., Tokyo, Japan).

### Data acquisition

The RNA-seq data were obtained from the Cancer Genome Atlas (TCGA) database (http://cancergenome.nih.gov), the Chinese Glioma Genome Atlas (CGGA, www.cgga.org), and the Gene Expression Omnibus (GEO) dataset. The independent dataset from GSE4290 was included in this study. The expression levels for each gene were calculated as transcripts per million values, which were defined by RSEM. GO analysis was performed using the Database for Annotation, Visualization, and Integrated Discovery (http://david.abcc.ncrf.gov/) online tool[30]. Significantly enriched gene sets were investigated. miRanda[55] and TargetScan[56] were utilized for miR-205-3p potential target screening.

### Transfection of glioma cells

For transfection, glioma cells were cultured in 6-well plates at $5 \times 10^5$ cells/wells and incubated in a 37 °C, 5% $CO_2$ humidified atmosphere. After 24 h, linc00645 siRNA and negative control (NC) siRNA (50 µM each), miRNA mimics and inhibitor (200 pmol each) from GenePharma (Shanghai, China) were transfected into cells using Lipofectamine 2000 (Invitrogen; Thermo Fisher Scientific, Carlsbad, CA, USA) according to the manufacturer's instructions. Cells were starved in serum-free medium for 4 h before medication and were continued in culture for 48 h. The siRNA sequences are listed in Table 2. The overexpression plasmid of linc00645 was synthesized into the pcDNA3.1(+) vectors. The psiCHECK2 dual luciferase vector was obtained from Promega (Madison, WI, USA).

### Western blot analysis

Cell lysates were collected by RIPA protein extraction buffer (Beyotime Institute of Biotechnology, Beijing, China) with protease inhibitor cocktail (Roche, Basel,

**Table 2 siRNA sequences**

| siRNA sequences | |
| --- | --- |
| NC-sense | UUCUCCGAACGUGUCACGUTT |
| NC-antisense | ACGUGACACGUUCGGAGAATT |
| si-Linc 1#-sense | GGAGUGAGAUGUCAAAUAACA |
| si-Linc 1#-antisense | UUAUUUGACAUCUCACUCCAU |
| si-Linc 2#-sense | UGGAUGAAAUAUUAGUUAAGU |
| si-Linc 2#-antisense | UUAACUAAUAUUUCAUCCAUA |
| si-Linc 3#-sense | CUUUAUGGAUGAAAUAUUAGU |
| si-Linc 3#-antisense | UAAUAUUUCAUCCAUAAAGGU |

### Table 3 Primary antibodies used for western blot analysis

| Antibodies | Species | Manufacture | Catalog# | Dilution |
| --- | --- | --- | --- | --- |
| E-cadherin | Rabbit | Proteintech | 20874-1-AP | 1:500 |
| Vimentin | Rabbit | Proteintech | 20874-1-AP | 1:1000 |
| N-cadherin | Rabbit | Proteintech | 22018-1-AP | 1:500 |
| Snail | Rabbit | Proteintech | 22018-1-AP | 1:500 |
| ZEB1 | Rabbit | Proteintech | 22018-1-AP | 1:1000 |
| Bcl-2 | Rabbit | Proteintech | 12789-AP | 1:1000 |
| Bax | Rabbit | Proteintech | 50599-2-lg | 1:500 |
| CD133 | Rabbit | Proteintech | 18470-1-AP | 1:50 |
| Bmi1 | Rabbit | Proteintech | 10832-1-AP | 1:50 |
| OCT4 | Rabbit | Proteintech | 11263-1-AP | 1:50 |
| SOX2 | Rabbit | Proteintech | 11064-1-AP | 1:50 |
| Nanog | Rabbit | Proteintech | 14295-1-AP | 1:50 |
| GFAP | Rabbit | Proteintech | 16825-1-AP | 1:20 |
| Nestin | Rabbit | Proteintech | 19483-1-AP | 1:20 |
| β-actin | Mouse | Proteintech | 60008-1-lg | 1:1000 |

### Table 4 Primers for qRT-PCR

| Primers for qRT-PCR | |
| --- | --- |
| Linc00645-F | CAGAGGTGGTGCCTTGACAT |
| Linc00645-R | ATATCCTCTGTGGCCCATGC |
| E-cadherin-F | CAAGCTATCCTTGCACCTCAG |
| E-cadherin-R | GCATCAGAGAACTCATCTTC |
| Vimentin-F | GGACCAGCTAACCAACGACA |
| Vimentin-R | AAGGTCAAGACGTGCCAGAG |
| Snail-F | CTCGGACCTTCTCCGAATG |
| Snail-R | AAGTCCTGTGGGGCTGATG |
| ZEB1-F | AAGTGGCGGTAGATGGTAATGT |
| ZEB1-R | ATGAAGACTGATGGCTGAAAT |
| GAPDH-F | CACCCACTCCTCCACCTTTG |
| GAPDH-R | CCACCACCCTGTTGCTGTAG |
| miR-205-3p-F | CTTGTCCTTCATTCCACCGGA |
| miR-205-3p-R | TGCCGCCTGAACTTCACTCC |
| U6-F | CTCGCTTCGGCAGCACA |
| U6-R | AACGCTTCACGAATTTGCGT |

Switzerland). Cell lysates were separated on 10% sodium dodecyl sulfate-polyacrylamide gel electrophoresis gel and transferred onto a polyvinylidene fluoride membrane (EMD Millipore Billerica, MA, USA). The membrane was then incubated with specific primary antibodies at 4 °C overnight (Table 3). Horseradish peroxidase-conjugated anti-mouse or anti-rabbit secondary antibody was added separately. The bands were captured using the Chemi-Doc™ MP Imaging System (Bio-Rad Laboratories, Inc., Hercules, CA, USA).

### qRT-PCR analysis

Total RNA was extracted from cells and tissues using the High Pure RNA Isolation Kit (Roche) and reverse transcription was performed with the PrimeScript® RT Reagent Kit Perfect Real Time (Takara, Dalian, China). qRT-PCR was conducted to detect mRNA, miRNA, and lncRNA by using the Takara's SYBR Premix Ex Taq™ II (Tli RNaseH Plus) according to the manufacturer's instructions. The results were normalized to the expression of GAPDH. Briefly, RNA was reverse transcribed (RT) using a cDNA kit in combination with a stem–loop primer for miRNA-205-3p. For miRNA quantification, the U6 gene was used as an internal control. The specific primer sequences are presented in Table 4. Subsequently, the assay was performed on a CFX96TM Real-Time System (Bio-Rad Laboratories, Inc.). The $2^{-\triangle\triangle Cq}$ method was used for quantification and fold-change for target genes was normalized by internal control.

### Isolation of cytoplasmic and nuclear RNA

Cytoplasmic and nuclear RNA were collected and purified by using the PARIS Kit (Life Technologies, Carlsbad, CA, USA) according to the manufacturers' instructions.

### Cell proliferation and colony formation assay

Cell viability was detected using a cell proliferation kit (Beyotime Institute of Biotechnology). Cells were seeded into 96-well plates at a density of 2000 cells/well. Following transfection with si-Linc 1#, 2#, 3# and a negative control (si-NC), 20 μl of MTT reagent was added to each well and then incubated for 4 h at 37 °C. The cell proliferation curves were measured at a wavelength of 570 nm at each indicated time point. Experiments were performed in triplicate.

For the colony formation assay, ~200 cells were cultured in 6-well plates after transfection for 48 h and maintained in 10% fetal bovine serum (FBS) at 37 °C for 12 days. After this, the colonies were fixed with 4% polyoxymethylene and stained with a hematoxylin and eosin (H&E) Staining Kit (Beyotime Institute of Biotechnology). The colony formation ratio was manually calculated.

### Flow cytometry analysis

Apoptosis assay was conducted using the FITC/ Annexin V Apoptosis Detection Kit (BD Biosciences, Franklin Lakes, NJ, USA). Cells were collected via trypsinization and washed twice with ice-cold phosphate-

buffered saline (PBS). Then, $1 \times 10^6$ cells/ml were resuspended in 1× binding buffer and 5 μL FITC Annexin V and 5 μl propidium iodide (PI) were added. The cells were analyzed by flow cytometry (FACScan; BD Biosciences) with CellQuest software 5.2 (BD Biosciences). All samples were assayed in triplicate.

### Immunofluorescence staining

Cells were fixed with 4% paraformaldehyde for 20 min and 0.1% Triton X-100 for 5 min. The samples were washed and blocked with 5% bovine serum albumin in PBS for 1 h and incubated with primary antibodies against vimentin (1:50, ProteinTech) at 4 °C overnight, followed by incubation with fluorescence-labeled rabbit secondary antibody (1:100, ProteinTech) for 1 h at room temperature. The nuclei were stained with DAPI for 10 min and examined using a fluorescence microscope (Nikon Corporation).

### Transwell assay and wound healing assay

Invasion assays were conducted using Corning chambers (Corning Life Sciences, Bedford, MA, USA). Cell suspensions were harvested 24 h after transfection and $5 \times 10^4$ cells in serum-free media were added into the upper chambers, which were coated with Matrigel (Sigma-Aldrich; Merck KGaA), while media containing 20% FBS were added into the lower chamber. The cells were incubated for 24 h at 37 °C. Cells remaining on the upper surface of the membrane were gently removed with a cotton swab, and cells that had invaded through the membrane were stained with methanol and H&E, before being counted in 4 random fields at a magnification of ×100.

For the wound-healing assay, transfected cells were seeded onto six-well plates and cultured overnight. Wounds were created by scratching the cell layer with a sterile 200 μl pipette tip, followed by washing with PBS. Cells were cultured with media containing 2% FBS for another 24 h and images were captured under a microscope. Both experiments were independently performed in triplicate.

### Luciferase reporter assay

To investigate whether miR-205-3p directly binds to the linc00645 3′ untranslated region (UTR), dual luciferase reporter assays were conducted. The psiCHECK2 vector (GeneChem, Shanghai, China) was employed to construct linc00645 3′UTR-containing reporter plasmids. Cells were co-transfected with psiCHECK2-linc-wild-type (WT), psiCHECK2-linc-mutant (MUT), psiCHECK2-ZEB1-3′UTR-WT or psiCHECK2-ZEB1-3′UTR-MUT reporter plasmids and miR-205-3p NC mimics. After transfection, the cells were lysed and subjected to luciferase assays using the Dual-Luciferase Reporter Assay

System (Promega Corporation), according to the manufacturer's instructions. Data were normalized to *Renilla* luciferase activity.

### Anti-AGO2 RIP assay

RIP assay was performed using the Magna RIP RNA-Binding Protein Immunoprecipitation (RIP) Kit (EMD Millipore). U251 and T98G cells transiently transfected with miR-205-3p were harvested using RIP lysis buffer and 100 μl of the cell lysate was employed for RIP experiments using an anti-AGO2 antibody (Abcam, Cambridge, MA, USA) according to the manufacturer's instructions. The beads were attracted by a magnetic separator, and samples were treated with proteinase K. The RNA fraction isolated by RIP was subjected to qRT-PCR analysis to identify the direct binding between linc00645 and miR-205-3p.

### In vivo experiments

Four-week-old female BALB/c nude mice were obtained from Vital River Laboratory Animal Technology (Beijing, China), were kept under standard conditions (15–20 g). Luciferase lentivirus of linc00645-shRNA or NC-shRNA were purchased from GeneChem (Shanghai, China). Then U251 cells were stable transfected with luciferase lentivirus. Subsequently, cells ($5 \times 10^5$ cells/mouse in 3 μL) were intracranially injected into the mice ($n = 7$ per group) using a stereotactic instrument. After 30 days, tumor growth were measured by bioluminescence imaging (photons/s/$cm^2$/sr) using Bruker In-Vivo FX PRO Imaging System (Bruker, Germany). After 40 days, the mice were anesthetized using isoflurane and sacrificed, then the tumors were excised. Then the tumor tissues were stored at −80 °C or fixed in 4% paraformaldehyde, and then histologically analyzed with H-E staining. All applicable international, national and/or institutional guidelines or the care and use of animals were followed. These procedures were displayed approval by the Institutional Review Board of Harbin Medical University.

### Statistical analysis

Statistical analyses were performed using SPSS v.19.0 (IBM Corp., Armonk, NY, USA). Data are presented as the mean ± standard deviation. Heat maps were constructed using HEMI 1.0 software. The correlation between linc00645 expression and the clinicopathological characteristics of patients with glioma was analyzed using the $\acute{y}^2$ test or Fisher's exact test. Survival curves were drawn using the log-rank test with GraphPad Prism 5.0 (GraphPad Software, Inc., La Jolla, CA, USA). The independent Student's *t* test was used to analyze the statistical significance between two groups and one-way ANOVA with post hoc Tukey's test was applied to test for differences among at least three groups to obtain individual

P values followed by ANOVA. The association of the expression of linc00645 with miR-205-3p, E-cadherin, Vimentin, N-cadherin, and ZEB1 was analyzed using Pearson's correlation. A P value < 0.05 was considered to indicate a statistically significant difference.

### Author details
[1]Department of Neurosurgery, Harbin Medical University Cancer Hospital, Harbin, Heilongjiang 150001, P.R. China. [2]Laboratory of Medical Genetics, Harbin Medical University, Harbin, Heilongjiang 150001, P.R. China. [3]Key Laboratory of Medical Genetics (Harbin Medical University), Heilongjiang Higher Education Institutions, Harbin, Heilongjiang 150001, P.R. China

### Authors' contributions
C.L. designed and performed the experiments, analyzed and interpreted data, and wrote the paper; H.Z., W.H., and H.B. performed the experiments, analyzed the data, and edited the paper; J.X. and W.C. designed and performed the experiments; P.L. and H.S. designed the experiments and critically reviewed the paper; Y.G. analyzed the data.

### Conflict of interest
The authors declare that they have no conflict of interest.

### Publisher's note
Springer Nature remains neutral with regard to jurisdictional claims in published maps and institutional affiliations.

**Supplementary Information** accompanies this paper at (https://doi.org/10.1038/s41419-019-1948-8).

### References
1. Khasraw, M., Ameratunga, M. S., Grant, R., Wheeler, H. & Pavlakis, N. Anti-angiogenic therapy for high-grade glioma. *Cochrane Database Syst. Rev.* **9**, CD008218 (2014).
2. Wang, J., Su, H. K., Zhao, H. F., Chen, Z. P. & To, S. S. Progress in the application of molecular biomarkers in gliomas. *Biochem. Biophys. Res. Commun.* **1**, 1–4 (2015).
3. Bastien, J. I., McNeill, K. A. & Fine, H. A. Molecular characterizations of glioblastoma, targeted therapy, and clinical results to date. *Cancer* **4**, 502–516 (2015).
4. Ombrato, L. & Malanchi, I. The EMT universe: space between cancer cell dissemination and metastasis initiation. *Crit. Rev. Oncog.* **5**, 349–361 (2014).
5. Hay, E. D. An overview of epithelio-mesenchymal transformation. *Acta Anat.* **1**, 8–20 (1995).
6. Thiery, J. P., Acloque, H., Huang, R. Y. & Nieto, M. A. Epithelial-mesenchymal transitions in development and disease. *Cell* **5**, 871–890 (2009).
7. Kahlert, U. D., Nikkhah, G. & Maciaczyk, J. Epithelial-to-mesenchymal (-like) transition as a relevant molecular event in malignant gliomas. *Cancer Lett.* **2**, 131–138 (2012).
8. Baum, B., Settleman, J. & Quinlan, M. P. Transitions between epithelial and mesenchymal states in development and disease. *Semin. Cell Dev. Biol.* **3**, 294–308 (2008).
9. Asiedu, M. K., Ingle, J. N., Behrens, M. D., Radisky, D. C. & Knutson, K. L. TGFbeta/TNF (alpha)-mediated epithelial-mesenchymal transition generates breast cancer stem cells with a claudin-low phenotype. *Cancer Res.* **13**, 4707–4719 (2011).
10. Wang, Y., Shi, J., Chai, K., Ying, X. & Zhou, B. P. The role of Snail in EMT and tumorigenesis. *Curr. Cancer Drug Targets* **9**, 963–972 (2013).
11. Wong, T. S., Gao, W. & Chan, Y. W. Transcription regulation of E-cadherin by zinc finger E-box binding homeobox proteins in solid tumors. *Biomed. Res. Int.* **1**, 921564 (2014).
12. Novikova, I. V., Hennelly, S. P., Tung, C. S. & Sanbonmatsu, K. Y. Rise of the RNA machines: exploring the structure of long non-coding RNAs. *J. Mol. Biol.* **19**, 3731–3746 (2013).
13. Batista, P. J. & Chang, H. Y. Long noncoding RNAs: cellular address codes in development and disease. *Cell* **6**, 1298–1307 (2013).
14. Martin, S. et al. Multiple knockout mouse models reveal lincRNAs are required for life and brain development. *Elife* **12**, e01749 (2013).
15. Han, Y. et al. Tumor-suppressive function of long noncoding RNA MALAT1 in glioma cells by downregulation of MMP2 and inactivation of ERK/MAPK signaling. *Cell Death Dis.* **3**, e2123 (2016).
16. Gupta, R. A. et al. Long non-coding RNA HOTAIR reprograms chromatin state to promote cancer metastasis. *Nature* **729**, 1071–1076 (2010).
17. Prensner, J. R. et al. The long noncoding RNA SChLAP1 promotes aggressive prostate cancer and antagonizes the SWI/SNF complex. *Nat. Genet.* **11**, 1392–1398 (2013).
18. Kotake, Y. et al. Long non-coding RNA ANRIL is required for the PRC2 recruitment to and silencing of p15INK4B tumor suppressor gene. *Oncogene* **16**, 1956–1962 (2011).
19. Han, Y., Liu, Y., Gui, Y. & Cai, Z. Long intergenic non-coding RNA TUG1 is overexpressed in urothelial carcinoma of the bladder. *J. Surg. Oncol.* **5**, 555–559 (2013).
20. Li, T. et al. Upregulation of long noncoding RNA ZEB1-AS1 promotes tumor metastasis and predicts poor prognosis in hepatocellular carcinoma. *Oncogene* **12**, 575–1584 (2016).
21. Jia, L., Tian, Y., Chen, Y. & Zhang, G. The silencing of LncRNA-H19 decreases chemoresistance of human glioma cells to temozolomide by suppressing epithelial-mesenchymal transition via the Wnt/β-Catenin pathway. *Onco Targets Ther.* **11**, 313–321 (2018).
22. Zhang, S. et al. Long non-coding RNA HOTTIP promotes hypoxia-induced epithelial-mesenchymal transition of malignant glioma by regulating the miR-101/ZEB1 axis. *Biomed. Pharmacother.* **95**, 711–720 (2017).
23. Zeng, J. et al. Knockdown of long noncoding RNA CCAT2 inhibits cellular proliferation, invasion, and EMT in glioma cells. *Oncol. Res.* **6**, 913–921 (2017).
24. Chen, B. J. et al. Transcriptome landscape of long intergenic non-coding RNAs in endometrial cancer. *Gynecol. Oncol.* **3**, 654–662 (2017).
25. Liang, R. et al. Analysis of long non-coding RNAs in glioblastoma for prognosis prediction using weighted gene co-expression network analysis, Cox regression, and L1-LASSO penalization. *Onco Targets Ther.* **12**, 157–168 (2018).
26. Salmena, L., Poliseno, L., Tay, Y., Kats, L. & Pandolfi, P. P. A ceRNA hypothesis: the Rosetta stone of a hidden RNA language? *Cell* **3**, 353–358 (2011).
27. Cesana, M. et al. A long noncoding RNA controls muscle differentiation by functioning as a competing endogenous RNA. *Cell* **2**, 358–369 (2011).
28. Karreth, F. A. et al. In vivo identification of tumor- suppressive PTEN ceRNAs in an oncogenic BRAF-induced mouse model of melanoma. *Cell* **2**, 382–395 (2011).
29. Qu, L. et al. Exosome-transmitted lncARSR promotes Sunitinib resistance in renal cancer by acting as a competing endogenous RNA. *Cancer Cell* **5**, 653–668 (2016).
30. Tang, J. et al. Molecular mechanisms of microRNAs in regulating epithelial-mesenchymal transitions in human cancers. *Cancer Lett.* **2**, 301–313 (2016).
31. Huang da, W., Sherman, B. T. & Lempicki, R. A. Systematic and integrative analysis of large gene lists using DAVID bioinformatics resources. *Nat. Protoc.* **1**, 44–57 (2009).
32. Robinson, M. D., McCarthy, D. J. & Smyth, G. K. edgeR: a Bioconductor package for differential expression analysis of digital gene expression data. *Bioinformatics* **26**, 139–140 (2010).
33. Nam, J. et al. Global analyses of the effect of different cellular contexts on microRNA targeting. *Mol. Cell* **6**, 1031–1043 (2014).
34. Yuan, J. H. et al. A long noncoding RNA activated by TGF-beta promotes the invasion-metastasis cascade in hepatocellular carcinoma. *Cancer Cell* **5**, 666–681 (2014).
35. Fan, Y. et al. TGF-beta-induced upregulation of malat1 promotes bladder cancer metastasis by associating with suz12. *Clin. Cancer Res.* **6**, 1531–1541 (2014).

36. Lee, J. Y. et al. Loss of the polycomb protein Mel-18 enhances the epithelial-mesenchymal transition by ZEB1 and ZEB2 expression through the down-regulation of miR-205 in breast cancer. *Oncogene* **10**, 1325–1335 (2014).

37. Hirata, H. et al. Long noncoding RNA MALAT1 promotes aggressive renal cell carcinoma through Ezh2 and interacts with miR-205. *Cancer Res.* **7**, 1322–1331 (2015).

38. Zhang, Y., Chen, Z., Li, M. J., Guo, H. Y. & Jing, N. C. Long non-coding RNA metastasis- associated lung adenocarcinoma transcript 1 regulates the expression of Gli2 by miR-202 to strengthen gastric cancer progression. *Biomed. Pharmacother.* **85**, 264–271 (2017).

39. Gregory, P. A. et al. The miR-200 family and miR-205 regulate epithelial to mesenchymal transition by targeting ZEB1 and SIP1. *Nat. Cell Biol.* **5**, 593–601 (2008).

40. Verhaak, R. G. W. et al. Integrated genomic analysis identifies clinically relevant subtypes of glioblastoma characterized by abnormalities in PDGFRA, IDH1, EGFR, and NF1. *Cancer Cell* **1**, 98–110 (2010).

41. Phillips, H. S. et al. Molecular subclasses of high-grade glioma predict prognosis, delineate a pattern of disease progression, and resemble stages in neurogenesis. *Cancer Cell* **3**, 157–173 (2006).

42. Zhang, P., Sun, Y. & Ma, L. ZEB1: at the crossroads of epithelial-mesenchymal transition, metastasis and therapy resistance. *Cell Cycle* **4**, 481–487 (2015).

43. Alves, C. P. et al. Brief Report: the lincRNA hotair is required for epithelial-to-mesenchymal transition and stemness maintenance of cancer cell lines. *Stem Cells* **12**, 2827–2832 (2013).

44. Chen, D. L. et al. Long noncoding RNA XIST expedites metastasis and modulates epithelial–mesenchymal transition in colorectal cancer. *Cell Death Dis.* **8**, e3011 (2017).

45. Rui, T., Gui, Z., Wang, Y. C., Mei, X. & Chen, S. Y. The long non-coding RNA GAS5 regulates transforming growth factor β (TGF-β)–induced smooth muscle cell differentiation via RNA Smad–binding elements. *J. Biol. Chem.* **34**, 14270–14278 (2017).

46. Lu, W. et al. Long non-coding RNA linc00673 regulated non-small cell lung cancer proliferation, migration, invasion and epithelial mesenchymal transition by sponging miR-150-5p. *Mol. Cancer* **1**, 118 (2017).

47. Li, C. et al. Long non-coding RNA XIST promotes TGF-β-induced epithelial-mesenchymal transition by regulating miR-367/141-ZEB2 axis in non-small-cell lung cancer. *Cancer Lett.* **418**, 185–195 (2018).

48. Jalali, S., Bhartiya, D., Lalwani, M. K., Sivasubbu, S. & Scaria, V. Systematic transcriptome wide analysis of lncRNA-miRNA interactions. *PLoS One* **2**, e53823 (2013).

49. Juan, L. et al. Potential roles of microRNAs in regulating long intergenic noncoding RNAs. *BMC Med. Genomics* **6**(Suppl 1), S7 (2013).

50. Hou, S. X. et al. Identification of microRNA-205 as a potential prognostic indicator for human glioma. *J. Clin. Neurosci.* **7**, 933–937 (2013).

51. De Moor, C. H., Meijer, H. & Lissenden, S. Mechanisms of translational control by the 3′ UTR in development and differentiation. *Semin. Cell Dev. Biol.* **1**, 49–58 (2005).

52. Hashiguchi, Y. et al. Tumor-suppressive roles of ΔNp63β-miR-205 axis in epithelial-mesenchymal transition of oral squamous cell carcinoma via targeting ZEB1 and ZEB2. *J. Cell Physiol.* **2**, 6565–6577 (2017).

53. Zaravinos, A. The regulatory role of microRNAs in EMT and cancer. *J. Oncol.* **2015**, 1–13 (2015).

54. Hu, H. et al. MiR-145 and miR-203 represses TGF-β-induced epithelial-mesenchymal transition and invasion by inhibiting SMAD3 in non-small cell lung cancer cells. *Lung Cancer* **97**, 87–94 (2016).

55. Madar, V. & Batista, S. A more practical approach for the benjamini-hochberg FDR controlling procedure for huge-scale testing problems. *Bioinformatics* **11**, 1716–1723 (2016).

56. Betel, D., Koppal, A., Agius, P., Sander, C. & Leslie, C. Comprehensive modeling of microRNA targets predicts functional non-conserved and non-canonical sites. *Genome Biol.* **8**, R90 (2010).